Biogeochemical weathering under ice: Size matters

J. L. Wadham,[1] M. Tranter,[1] M. Skidmore,[2] A. J. Hodson,[3] J. Priscu,[4] W. B. Lyons,[5] M. Sharp,[6] P. Wynn,[7] and M. Jackson[8]

Received 2 October 2009; revised 26 December 2009; accepted 3 March 2010; published 23 September 2010.

[1] The basal regions of continental ice sheets are gaps in our current understanding of the Earth's biosphere and biogeochemical cycles. We draw on existing and new chemical data sets for subglacial meltwaters to provide the first comprehensive assessment of sub-ice sheet biogeochemical weathering. We show that size of the ice mass is a critical control on the balance of chemical weathering processes and that microbial activity is ubiquitous in driving dissolution. Carbonate dissolution fueled by sulfide oxidation and microbial CO_2 dominate beneath small valley glaciers. Prolonged meltwater residence times and greater isolation characteristic of ice sheets lead to the development of anoxia and enhanced silicate dissolution due to calcite saturation. We show that sub-ice sheet environments are highly geochemically reactive and should be considered in regional and global solute budgets. For example, calculated solute fluxes from Antarctica (72–130 t yr^{-1}) are the same order of magnitude as those from some of the world's largest rivers and rates of chemical weathering (10–17 t km^{-2} yr^{-1}) are high for the annual specific discharge (2.3–4.1 × 10^{-3} m). Our model of chemical weathering dynamics provides important information on subglacial biodiversity and global biogeochemical cycles and may be used to design strategies for the first sampling of Antarctic Subglacial Lakes and other sub-ice sheet environments for the next decade.

Citation: Wadham, J. L., M. Tranter, M. Skidmore, A. J. Hodson, J. Priscu, W. B. Lyons, M. Sharp, P. Wynn, and M. Jackson (2010), Biogeochemical weathering under ice: Size matters, *Global Biogeochem. Cycles*, *24*, GB3025, doi:10.1029/2009GB003688.

1. Body

[2] Ice sheets cover 10% of the Earth's surface at present, rising to 30% during Quaternary glaciations and almost 100% coverage during ancient global glaciations [*Hoffman et al.*, 1998]. Satellite and geodetic data have begun to reveal the nature of ice sheet hydrological systems, demonstrating the rapid drainage of surface meltwater to the bed in Greenland [*Zwally et al.*, 2002; *Das et al.*, 2008] and the transfer of teraliter volumes of meltwater between Antarctic Subglacial Lakes [*Wingham et al.*, 2006; *Fricker et al.*, 2007]. Little is known, however, about the biogeochemical processes in these hydrologically dynamic systems. There is mounting evidence that the beds of glaciers and ice sheets are host to unique and diverse communities of microorganisms [*Sharp et al.*, 1999; *Skidmore et al.*, 2000; *Foght et al.*, 2004; *Wadham et al.*, 2004; *Bhatia et al.*, 2006; *Mikucki et al.*, 2009; *Lanoil et al.*, 2009]. Many of the organisms present beneath valley glaciers are thought to play an important role in mediating chemical weathering processes through the catalysis of sulfide oxidation reactions [*Bottrell and Tranter*, 2002; *Wadham et al.*, 2004; *Wynn et al.*, 2006] and the generation of CO_2 by respiration [*Wadham et al.*, 2004; *Tranter et al.*, 2005]. These chemical weathering processes may be critical to their survival through the release of organic carbon [*Wadham et al.*, 2004] and nitrogen and phosphorus [*Hodson et al.*, 2005] from the bedrock. There is currently a dearth of information regarding the biogeochemical processes in the more remote ice sheet environments. This missing information is central to determining the contribution of ice sheets to the Earth's global biogeochemical cycles and to global biodiversity [*Priscu et al.*, 2008].

[3] Chemical weathering beneath the ice sheets may have a global impact if the balance of dissolution processes is similar to that beneath valley glaciers. Recent works have hypothesized that the release of bioavailable iron from sediments in melting icebergs [*Raiswell et al.*, 2006, 2008, 2009] and in aqueous form in the glacial runoff [*Föllmi et al.*,

[1]Bristol Glaciology Centre, School of Geographical Sciences, University of Bristol, Bristol, UK.
[2]Department of Earth Sciences, Montana State University, Bozeman, Montana, USA.
[3]Department of Geography, University of Sheffield, Sheffield, UK.
[4]Department of Land Resources and Environmental Science, Montana State University, Bozeman, Montana, USA.
[5]Byrd Polar Centre, Ohio State University, Columbus, Ohio, USA.
[6]Department of Earth and Atmospheric Sciences, University of Alberta, Edmonton, Canada.
[7]The Lancaster Environment Centre, Lancaster University, Lancaster, UK.
[8]Glacier and Environmental Hydrology Section, Hydrology Department, Norwegian Water Resources and Energy Directorate, Oslo, Norway.

0886-6236/10/2009GB003688

2009] may be an important stimulant of ocean primary productivity, with potential negative feedback effects on climate via CO_2 drawdown. This iron is derived from sulfides present in the bedrock, which is continually exposed by subglacial comminution and, subsequently, is oxidized to produce reactive Fe(III) oxyhydroxides. Intense subglacial physical erosion also promotes high rates of detrital phosphorus export from glaciers with the potential to sustain downstream productivity [*Föllmi et al.*, 2009]. Others have suggested that anoxia generated beneath the continental ice sheets may promote the production of methane after periods of ice advance and carbon burial. This is then released during glacial retreat with the potential to stimulate greenhouse warming [*Skidmore et al.*, 2000; *Weitemeyer and Buffett*, 2008; *Wadham et al.*, 2008].

[4] Syntheses of glacial chemical weathering to date have used the chemical composition of bulk runoff from valley glaciers to infer chemical dissolution processes beneath ice sheets [*Sharp et al.*, 1995; *Anderson et al.*, 1997; *Hodson et al.*, 2000]. We argue that these studies failed to fully capture the variability of biogeochemical processes in subglacial environments, particularly long-residence time systems, because (1) mixing processes skew the chemical signature toward the larger-volume dilute channelized component and (2) subglacial meltwater chemistry becomes modified in ice-marginal environments [*Brown et al.*, 1994]. Data from valley glaciers are difficult to scale up to ice sheets, where meltwater residence times and the degree of isolation from the atmosphere are very different. Pure subglacial meltwaters have been sampled for chemical parameters from just a few glaciers worldwide because of the logistical constraints of obtaining samples. We draw on the full spectrum of these data sets and combine them with new ice sheet chemical data sets to provide the first assessment of biogeochemical processes beneath ice sheets.

2. Subglacial Data Sets and Data Analysis

[5] We use subglacial chemical data from eight ice masses differing in scale (Table 1 and Appendix A for unpublished methods), inferring that subglacial meltwater residence time scales approximately with the size of the ice mass and the degree of isolation from surface environments. The Haut Glacier d'Arolla (Switzerland, 6.3 km^2) and Engabreen (Norway, 40 km^2) are temperate glacier end-members. They have ice that is at the pressure melting point throughout during summer, and they have well-developed subglacial drainage systems. Midre Lovénbreen (5 km^2) is their "polythermal" counterpart, where the surface and margins of the glacier are below the pressure melting point, but parts of the bed are temperate. Finsterwalderbreen (Svalbard) is a medium-sized (~40 km^2) polythermal system, where surface cold ice reduces surface-to-bed hydrological connectivity, prolonging residence times. The largest and most isolated systems are the Bristol Glacier (Greenland Ice Sheet), Lake Vostok (East Antarctica: estimated residence time = 32,000 years; *Thoma et al.*, 2008) and the Kamb and Bindschadler ice streams (KIS and BIS, respectively, West Antarctica). On Greenland, surface meltwater penetrates the bed in the ablation zone. In the Antarctic cases, there is no surface meltwater penetration to the ice sheet bed. Hence, all meltwater derives from basal melting of the ice sheet base due to geothermal and frictional heating. This is anticipated to result in low meltwater fluxes and prolonged meltwater residence times. We also use Lake Vostok accretion ice data, derived from two separate data sets of waters that have frozen to the base of the Antarctic Ice Sheet above Lake Vostok [*DeAngelis et al.*, 2004] (Appendix A for unpublished methods). As for all data sets, we analyze the associations between ions rather than absolute ion concentrations. This minimizes issues associated with (differential) ion rejection during freezing for Vostok ice and the fact that the true lake water concentrations are consequently much higher than those in the accretion ice. Hence, although there may be considerable scatter in plots of one ion versus another, lines of best fit give the average chemical composition of the accretion ice regardless of freezing effects on ion ratios.

[6] We analyze four primary chemical indices. First and second are the concentrations of SO_4^{2-} and HCO_3^- that reflect the relative dominance of several major chemical weathering mechanisms, sulfide oxidation, and the sum of carbonation, carbonate hydrolysis, and carbonate dissolution, respectively [equations (1)–(4)] [*Holland*, 1978].

$$4FeS_{2(s)} + 14H_2O_{(l)} + 15O_{2(aq)} \leftrightarrow 16H^+_{(aq)} + 8SO^{2-}_{4(aq)} + 4Fe(OH)_{3(s)} \quad (1)$$

$$CO_{2(g)} + H_2O_{(l)} \leftrightarrow 2HCO^-_{3(aq)} \leftrightarrow HCO^-_{3(aq)} + H^+_{(aq)} \quad (2)$$

$$CaCO_{3(s)} + H_2O_{(l)} \leftrightarrow Ca^{2+}_{(aq)} + HCO^-_{3(aq)} + OH^-_{(aq)} \quad (3)$$

$$CaCO_{3(s)} + H^+_{(aq)} \leftrightarrow Ca^{2+}_{(aq)} + HCO^-_{3(aq)} \quad (4)$$

Third is the ($*Ca^{2+} + *Mg^{2+}$) concentration, which is used as a bulk indicator of carbonate dissolution. Fourth is the concentration of ($*Na^+ + *K^+$), indicative of silicate dissolution [*Holland et al.*, 1978]. All cation and sulfate concentrations are corrected for their sea salt– and snowpack-derived components, respectively, using Cl^- concentrations and ratios of each species to Cl^- in either seawater (cations) or locally sampled snow (SO_4^{2-}). The snowpack sulfate contributions in the Vostok data are derived from mean ratios in the meteoric ice immediately above the accretion ice (Appendix A). Sea salt ratios are used for all ion corrections in BIS and KIS. The residual crustal-derived component is denoted with an asterisk (*).

[7] We focus on the gradients and intercepts observed for the lines of best fit for associations of HCO_3^- versus $*SO_4^{2-}$ and $*Ca^{2+} + *Mg^{2+}$ versus $*SO_4^{2-}$. We present the mean ratios of $HCO_3^-/*SO_4^{2-}$ and $*Ca^{2+} + *Mg^{2+}/*SO_4^{2-}$ for the KIS and BIS pore waters owing to the small number of data points. The primary focus on the associations between ions rather than on the absolute ion concentrations minimizes the issues associated with ion rejection during freezing for Vostok ice and the fact that the true lake water concentrations are consequently much higher than those in the accretion ice. Figure 1 displays the HCO_3^- versus $*SO_4^{2-}$ associations for

Table 1. Details of Subglacial Data Sets

Glacier Name	Bedrock Lithology	Size (km^2)	Sample Details	Thermal Regime	Reference If Published
Lake Vostok, Antarctica	Unknown	16,820[27]	Accretion ice	Polythermal	This paper
Kamb and Bindschadler ice streams, West Antarctic Ice Sheet	Plio-Pleistocene tills	306,000	Pore water extracted from soft sediments	Polythermal	*Sharp et al.* [1999] and *Siegert et al.* [2007]
Bristol Glacier, SW Greenland	Archean gneiss	60	Subglacial outburst meltwaters	Polythermal	This paper
Finsterwalderbreen, Svalbard	Precambrian carbonate, phyllite and quartzite; Permian sandstones, dolomites, and limestones; and Triassic-Cretaceous siltstones, sandstones, and shales	44	Subglacial upwelling	Polythermal	*Christner et al.* [2006] and *Raiswell et al.* [2008]
Midre Lovénbreen, Svalbard	Phyllites and quartzite, mica schist, marble, minor carbonate, and sandstone	5	Subglacial upwelling	Polythermal	1998–2000: this paper, 2002 data, and *Föllmi et al.* [2009]
Engabreen, N Norway	Metamorphic (gneiss and schist)	39.6	Subglacial intake pipes	Temperate	This paper
Haut Glacier d'Arolla, Switzerland	Amphibolite, greenschist, gabbro, quartz, feldspars, pyroxenes, mica, amphibole, cordierite, hematite, magnetite, and talc. Trace carbonates and sulfides.	6.3	Borehole waters	Temperate	*Raiswell et al.* [2006]

all data sets (excluding the KIS and BIS) and provides an example of the plots used for analysis. A wide range of gradients and intercepts are evident (Table 2), which can be used to identify the systematic trends in the dissolution processes between ice masses of different scale.

3. Chemical Weathering Processes Under Ice: A Predictive Framework

[8] The first reaction to occur on the wetting of the subglacial flour is hydrolysis, predominantly of calcite, which generates ~220 μeq L^{-1} of HCO_3^- and Ca^{2+} in line with the theoretical solubility of calcite in pure water at 0°C [equation (3)] [*Tranter et al.*, 2002a]. Because this reaction involves the rapid acquisition of HCO_3^- and $*Ca^{2+}$ in the absence of $*SO_4^{2-}$, the intercept in the plots of HCO_3^- versus $*SO_4^{2-}$ should be approximately 220 μeq L^{-1}. We note that the intercept values for Vostok accretion ice are artificially low because of the solute exclusion during freezing (Figure 1 and Table 2). Of the remaining data sets, approximately half display intercepts of >220 μeq L^{-1} in plots of HCO_3^- and $*Ca^{2+} + *Mg^{2+}$ versus $*SO_4^{2-}$ (Figure 2a and Table 1). This range of intercepts suggests an additional source of CO_2 to meltwaters. Acquisition of solute by carbonation reactions using atmospheric CO_2 in subglacial environments is negligible because these systems are out of direct contact with the atmosphere and often have high partial pressures of CO_2 because of the proton supply from sulfide oxidation and the inability of meltwaters to degas [*Tranter et al.*, 2002a, 2005; *Wadham et al.*, 1998]. Hence, we infer that the additional HCO_3^- is acquired via the generation of CO_2 during the microbial oxidation of organic carbon in subglacial sediments. A direct and significant association ($P = 0.01$, $r^2 = 0.83$) between the intercepts in plots of both HCO_3^- and $*Ca^{2+} + *Mg^{2+}$ versus $*SO_4^{2-}$ implies that most of this excess HCO_3^- is balanced by a similar quantity of $*Ca^{2+} + *Mg^{2+}$ (Figure 2a). A gradient of 0.79, Figure 2a further implies that, on average, 80% of microbial CO_2 dissolves calcite, with the remainder dissolving silicates. This is a maximum estimate of calcite dissolution because it does not account for the fact that minor amounts of $*Mg^{2+}$ and $*Ca^{2+}$ may be derived from silicates. It is consistent, however, with the reaction kinetics for both dissolution processes [*Tranter et al.*, 2002a]. The amount of microbial CO_2 is bedrock substrate-dependent, with the hard rock-bedded glacier systems (Arolla, Greenland, Engabreen, and Greenland Ice Sheet) displaying the lowest intercepts (Figure 2a). Higher intercepts for Finsterwalderbreen and Midre Lovénbreen are consistent with the drainage of subglacial meltwaters (via artesian upwellings) from sediment-rich environments [*Wadham et al.*, 1998], which are believed to dominate significant areas of the glacier bed and result from the erosion of underlying sedimentary rocks. These findings reveal that glaciers based on hard, less reactive bedrock constitute less favorable environments for microbial activity, which is consistent with observations elsewhere that subglacial microbial populations tend to correlate with sediment distributions [*Sharp et al.*, 1999].

[9] Subsequent to carbonate hydrolysis, subglacial waters may evolve via the oxidation of sulfide minerals continually

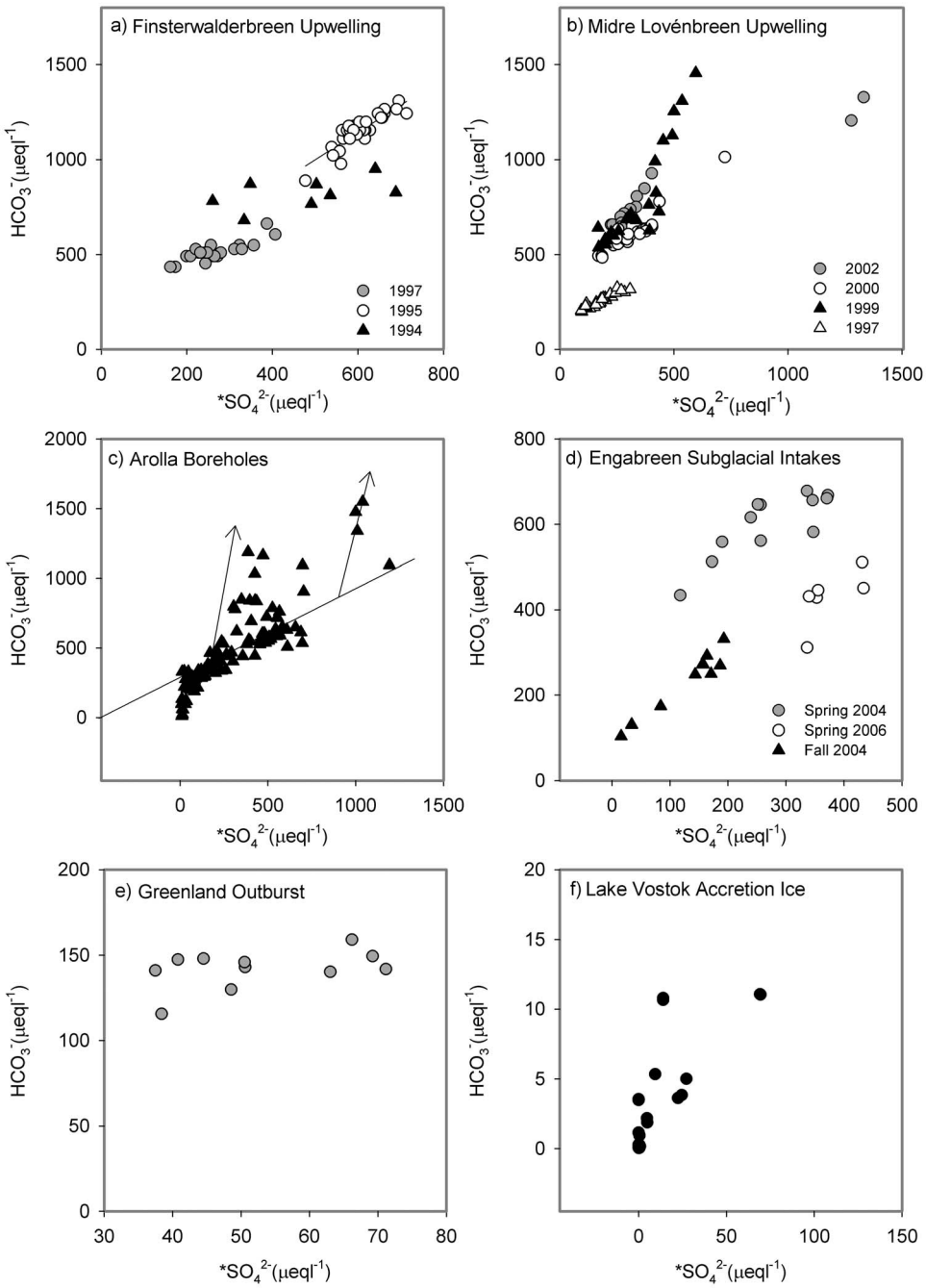

Figure 1. Associations between HCO_3^- and $*SO_4^{2-}$ for subglacial meltwaters. All associations presented are significant at the 99% confidence level, apart from the Greenland outburst data and the Finsterwalderbreen 1994 data for HCO_3^- versus $*SO_4^{2-}$ because of the low gradients and small number of data points. We include these data, but note that the gradients and intercept values have a high degree of error associated with them. We note that several water types (offshoots from the main Arolla borehole water trend and data from Finsterwalderbreen 1995; denoted in Figures 1a and 1c, respectively) display ratios of HCO_3^- relative to $*SO_4^{2-}$, which greatly exceed the theoretical ratio for sulfide oxidation/carbonate dissolution of 1:1. We contend that these alterations in gradient are not true chemical evolution trends and result from subglacial drainage evolution. These data points are excluded from subsequent discussion.

Table 2. Associations and Values for Individual Data Sets

	HCO_3^- versus $*SO_4^{2-}$	$*Ca^{2+} + *Mg^{2+}$ versus $*SO_4^{2-}$	Mean $*Ca^{2+} + *Mg^{2+}/*Na^+ + *K^+$
Haut Glacier d'Arolla (all data)	$y = 0.980 + 188$ ($n = 139$, $r^2 = 0.75$)	$y = 1.96x + 171$ ($n = 140$, $r^2 = 0.93$)	26.0 ($n = 152$)
Without offshoots	$y = 0.770 + 205$ ($n = 126$, $r^2 = 0.84$)	$y = 1.75x + 188$ ($n = 126$, $r^2 = 0.97$)	24.0 ($n = 138$)
Engabreen			
Spring 2004	$y = 0.72x + 405$ ($n = 14$, $r^2 = 0.7$)	$y = 2.00x + 174$ ($n = 14$, $r^2 = 0.97$)	4.70 ($n = 14$)
Fall 2004	$y = 1.13x + 87.3$ ($n = 10$, $r^2 = 0.94$)	$y = 2.10 + 97.0$ ($n = 10$, $r^2 = 0.9$)	18.0 ($n = 10$)
Spring 2006	$Y = 0.981x + 61.7$ ($n = 6$, $r^2 = 0.46$)	$y = 1.80x + 102$ ($n = 6$, $r^2 = 0.86$)	17.4 ($n = 6$)
Midre Lovénbreen			
Summer 1997	$y = 0.570x + 153$ ($n = 25$, $r^2 = 0.89$)	$y = 1.33x + 172$ ($r^2 = 0.68$)	8.65 ($n = 25$)
Summer 1999	$y = 1.91x + 151$ ($n = 22$, $r^2 = 0.8$)	$y = 1.78x + 2.67$ ($n = 22$, $r^2 = 0.82$)	10.4 ($n = 22$)
Summer 2000	$y = 0.868 + 334$ ($n = 26$, $r^2 = 0.9$)	$y = 1.71 + 307$ ($n = 26$, $r^2 = 0.98$)	10.1 ($n = 26$)
Summer 2002	$y = 0.540 + 569$ ($n = 13$, $r^2 = 0.92$)	$y = 1.45x + 444$ ($n = 13$, $R = 0.99$)	6.70 ($n = 13$)
Finsterwalderbreen			
Summer 1994	$y = 0.280x + 686$ ($n = 8$, $r^2 = 0.27$)	$1.283x + 619$ ($n = 8$, $r^2 = 0.94$)	11.8 ($n = 8$)
Summer 1995	$y = 1.44x + 278$ ($n = 32$, $r^2 = 0.77$)	$y = 1.82x + 379$ ($n = 33$, $r^2 = 0.84$)	5.70 ($n = 33$)
Summer 1997	$y = 0.660x + 340$ ($n = 21$, $r^2 = 0.7$)	$1.34x + 415$ ($n = 22$, $r^2 = 0.81$)	12.0 ($n = 19$)
Bristol Glacier, Greenland			
Summer 1999	$y = 0.175x + 135$ ($n = 14$, $r^2 = 0.08$)	$y = 1.24x + 86.0$ ($n = 14$, $r^2 = 0.8$)	3.40 ($n = 14$)
Lake Vostok	$y = 0.157x + 1.25$ ($n = 29$, $r^2 = 0.62$)	$y = 0.95x + 0.790$ ($n = 29$, $r^2 = 0.99$)	4.95 ($n = 5$)
Kamb Ice Stream (mean values reported)	0.240 ($n = 3$)	0.550 ($n = 3$)	0.970 ($n = 3$)
Bindschadler Ice Stream (mean values reported)	0.120 ($n = 7$)	0.600 ($n = 7$)	1.01 ($n = 7$)

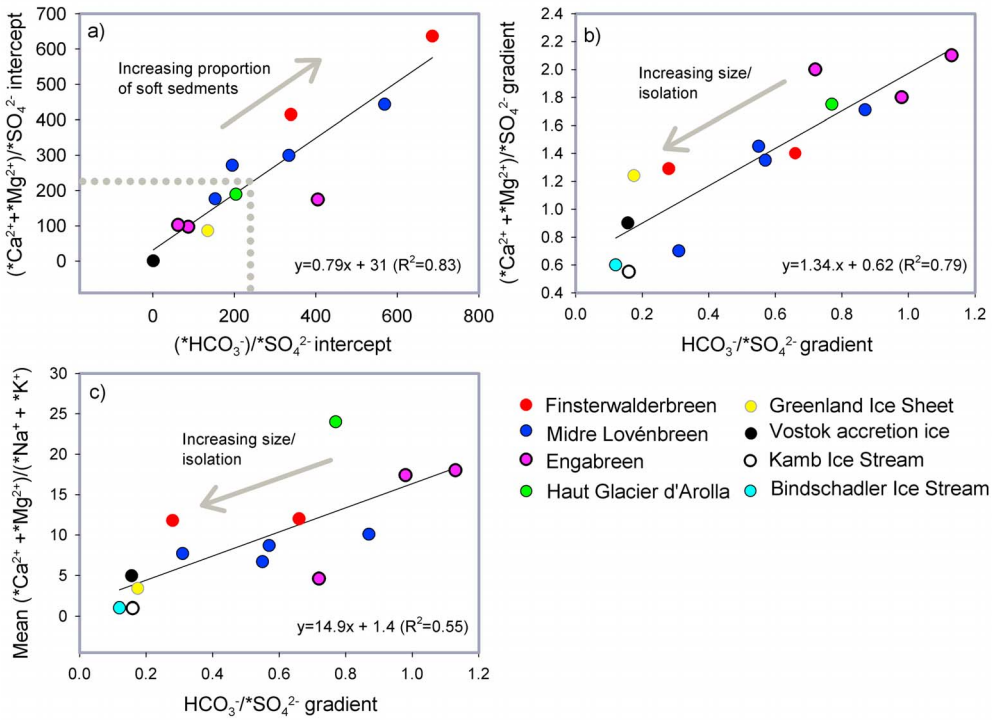

Figure 2. (a) Associations between intercepts for plots of $*Ca^{2+} + *Mg^{2+}$ versus $*SO_4^{2-}$ and HCO_3^- versus $*SO_4^{2-}$, where the maximum possible intercept because of carbonate hydrolysis is shown at 220 μeq L^{-1}. (b) Gradients derived from plots of $*Ca^{2+} + *Mg^{2+}$ versus $*SO_4^{2-}$ and HCO_3^- versus $*SO_4^{2-}$. (c) Association between the mean $*Ca^{2+} + *Mg^{2+}/*Na^+ + *K^+$ and gradients in plots of HCO_3^- versus SO_4^{2-}. The associations from which lines of best fit were compiled were all significant at the 99% confidence limit apart from the Greenland outburst data and the Finsterwalderbreen 1994 data (Figure 1). Associations presented in Figures 2a–c are all significant at the 95% confidence interval.

regenerated by glacial comminution and oxidized microbially under both oxic and anoxic conditions [*Tranter et al.*, 2002a, 2002b; *Bottrell and Tranter*, 2002; *Wadham et al.*, 2004; *Wynn et al.*, 2006]. Sulfide oxidation provides protons for carbonate and silicate dissolution [equations (5) and (6)]. Sulfate is produced during both coupled sulfide oxidation/carbonate dissolution and sulfide oxidation/silicate dissolution. HCO_3^- is generated during coupled sulfide oxidation/carbonate dissolution [equation (5)] but not during sulfide oxidation/silicate dissolution [equation (6)].

$$4FeS_{2(s)} + 16Ca_{1-x}(Mg_x) + 14H_2O_{(l)} + 15O_{2(aq)} \leftrightarrow 16(1-x)Ca^{2+}_{(aq)} + 16xMg^{2+}_{(aq)} + 16HCO^-_{3(aq)} + 8SO^{2-}_{4(aq)} + 4Fe(OH)_{3(s)} \quad (5)$$

(Mg⁻)Calcite

$$4FeS_{2(s)} + 16Na_{1-x}K_xAlSi_3O_{8(s)} + 86H_2O_{(l)} + 15O_{2(aq)} \leftrightarrow 16(1-x)Na^+_{(aq)} + 16xK^+_{(aq)} + 8SO^{2-}_{4(aq)} + 4Al_4Si_4O_{10}(OH)_{8(s)} + 32H_4SiO_{4(aq)} + 4Fe(OH)_{3(s)} \quad (6)$$

alkali feldspar — kaolinite

The stoichiometry of the coupled sulfide oxidation/carbonate dissolution generates SO_4^{2-} in molar equivalent ratios of 1:1 with respect to HCO_3^- and 2:1 with respect to $*Ca^{2+} + *Mg^{2+}$. Hence, gradients of ~1 and 2 in plots of HCO_3^- versus $*SO_4^{2-}$ and $*Ca^{2+} + *Mg^{2+}$, respectively, reflect complete coupling of sulfide oxidation and carbonate dissolution (via anoxic or oxic mechanisms; *Tranter et al.* [2002a]), whereas gradients of <1 and <2, respectively, suggest that some protons from sulfide oxidation dissolve silicate minerals, liberating Na^+ and K^+ [*Tranter et al.*, 2002a]. Most subglacial meltwaters display gradients of <1 and <2, respectively (Figure 2b), suggesting that protons generated from the oxidation of sulfide minerals are indeed used in variable degrees to dissolve silicate minerals. In support of this contention is the direct and significant association (r^2 = 0.48, P = 0.01) between mean ratios of $*Ca^{2+} + *Mg^{2+}/*Na^+*K^+$ and gradients of HCO_3^- versus $*SO_4^{2-}$ (Figure 2c). Figures 2b and c also indicate that the degree of coupled silicate dissolution and sulfide oxidation is directly related to the scale of the ice mass and to the degree of subglacial isolation. The temperate valley glaciers (Engabreen, Arolla), with well-developed subglacial drainage networks, display gradients close to the theoretical values of 1 and 2, respectively. The middle-scale polythermal system, Finsterwalderbreen, displays low to intermediate gradients of 0.2–0.66 and 1.3–1.4, respectively, while Midre Lovénbreen exhibits a range of values that largely reflect changing hydrological conditions between years. The lowest gradients of HCO_3^- and $*Ca^{2+} + *Mg^{2+}$ versus $*SO_4^{2-}$ are evident in the four sub-ice sheet meltwaters (0.1–0.2 and 0.6–1.2, respectively). The spatial patterns in mean ratios of $*Ca^{2+} + *Mg^{2+}/*Na^+*K^+$ also map with the scale of the ice mass (Figure 2c), with sub-ice sheet meltwaters displaying the lowest ratios (<5). Estimates of meltwater residence times beneath Antarctica and Greenland are wide ranging (from days in parts of Greenland [Wadham, unpublished data, 2009] to 10^4 years for Lake Vostok [*Thoma et al.*, 2008]) but are likely to be orders of magnitude higher than for valley glaciers because surface melt inputs are absent over large parts of the ice sheets. The most likely explanation for the enhanced silicate dissolution in these remote, long-residence time systems is the attainment of saturation with respect to calcite, but calcite exhaustion may also occur.

[10] These assertions suggest that the dominant control on subglacial meltwater chemical composition is the scale of the ice mass. We contend that bedrock lithology exerts a second-order effect. For example, meltwaters from all seven ice masses display significant concentrations of Ca^{2+} as the dominant cation and HCO_3^- and SO_4^{2-} as the primary anions, supporting the assertion that sulfide and calcite minerals are present in most (noncarbonate) bedrock types and dominate chemical dissolution because of their high geochemical reactivity [*Anderson*, 2007]. The smaller temperate systems, Engabreen and Haut Glacier d'Arolla, have silicate-rich bedrock lithologies, yet their subglacial chemical composition principally reflects the action of coupled sulfide oxidation/carbonate dissolution. Our data do show, however, that bedrock affects meltwater chemistry by controlling the development of a suitable microbial substrate. Softer sedimentary bedrocks are likely to give rise to thicker, more widespread, subglacial sedimentary deposits, which, in turn, provide a suitable habitat for microbial communities. Hence, meltwaters from these environments display higher proportions of microbially generated CO_2 and higher intercepts for lines of best fit in the plots of HCO_3^- and $*Ca^{2+} + *Mg^{2+}$ against $*SO_4^{2-}$ (e.g., Finsterwalderbreen). In contrast, glaciers based on less erodible substrates (e.g., continental shield bedrock) may have more localized and thinner subglacial debris deposits and, hence, less microbial activity.

4. Wider Impacts of Sub-Ice Sheet Chemical Weathering

[11] The above synthesis can be used as a framework for evaluating the likely evolution of meltwaters beneath ice sheets, including the Antarctic Subglacial Lakes. Our findings have four significant implications. First, microbially generated CO_2 is an important driver of chemical weathering in many subglacial environments, as indicated by the high intercepts in the plots of HCO_3^- and $*Ca^{2+} + *Mg^{2+}$ versus $*SO_4^{2-}$ (Figure 2a). We calculate that this microbially derived HCO_3^- accounts for up to 19%–65% (mean = 36%, n = 5) of the total HCO_3^- and that 14%–37% (mean = 22%, n = 5) of the total solute is acquired using microbial CO_2 as a proton source (Appendix B). The assertion that microbial CO_2 drives significant subglacial chemical weathering counters a previous work, which has suggested that exhaustion of carbonic acid poses a limitation on the dissolution processes beneath glaciers [*Anderson*, 2007]. Our data further indicate that this microbial effect is greatest for glaciers overlying soft sediments and, therefore, could be

important in driving chemical dissolution beneath ice streams and outlet glaciers resting on deformable sediments. This is particularly true in Antarctica, where basal melt is the primary source of O_2 and CO_2 because there is a limited supply of these gases to the basal environment from surface melting.

[12] Second, the oxidation of both organic carbon and sulfide minerals strips oxygen from meltwaters, creating the potential for a diversity of redox conditions at ice sheet beds and highly anoxic conditions in the ice sheet interior. This corroborates what is already known about valley glaciers, where sulfides are oxidized anoxically by chemolithoautotrophs, with nitrate or Fe(III) as terminal electron acceptors [*Bottrell and Tranter*, 2002; *Wadham et al.*, 2004, 2007; *Wynn et al.*, 2006]. Our data compilation implies that sulfide oxidation continues to be important under ice sheets. Certainly, if SO_4^{2-} present in the KIS and BIS waters is derived from sulfide oxidation, it is impossible to generate the concentrations of sulfate observed (53 meq L^{-1}) without driving the system anoxic (e.g., 300–400 μeq L^{-1} of SO_4^{2-} can be produced from oxygen-saturated snowmelt at 0°C [*Tranter et al.*, 2002a]). Hence, it is likely indicated that organic carbon and sulfide minerals are being oxidized using alternative oxidizing agents to the atmospheric oxygen. If this is the case, then ice sheet beds may be a host to diverse syntrophic communities of microbes, adapted to local bed Eh/pH conditions, which are, in turn, perpetuated by this very microbial activity. This analysis lends strong support to the contention that sub-ice sheet environments may have been sites of methanogenesis during periods of glacial advance and organic carbon burial and were important sources of methane to the atmosphere during ice wastage [*Skidmore et al.*, 2000; *Weitemeyer and Buffett*, 2008; *Wadham et al.*, 2008]. It also supports recent contentions that bioavailable nanoparticulate iron (oxyhydroxides) can be generated beneath ice sheets in a similar way to that beneath valley glaciers and that continual regeneration of sulfide minerals by comminution keeps pace with oxidation processes [*Raiswell et al.*, 2006, 2008, 2009]. This is consistent with the amplification of 16S rRNA gene sequences that are closely related to species known to be involved in sulfur and iron oxidation from subglacial waters from Bench Glacier, AL [*Skidmore et al.*, 2005]; KIS basal sediments [*Lanoil et al.*, 2009]; and Vostok accretion ice [*Christner et al.*, 2006]. It lends powerful support to the idea that sediments released from ice sheets, via icebergs or proglacial sediment deposition, may have the potential to stimulate ocean primary production [*Raiswell et al.*, 2006, 2008, 2009; *Föllmi et al.*, 2009].

[13] Third, our data show that as scale and, hence, residence time/isolation increase, silicate mineral dissolution dominates as meltwaters attain saturation with respect to calcite. Because silicate minerals contain trace amounts of nitrogen (e.g., in micas and feldspars) and potassium (in feldspars and biotite) [*Holloway and Dahlgren*, 2002], their enhanced dissolution can supply subglacial environments with the nutrients required to sustain microbial life. The high concentrations (30 meq L^{-1}) of $*Na^+$ and $*K^+$ in the KIS and BIS pore waters are consistent with enhanced silicate dissolution [*Skidmore et al.*, 2010] and suggest that chemical weathering beneath Antarctic Ice Streams is highly aggressive, driven by sulfide oxidation and microbially produced CO_2. Consistent with these assertions is the morphology of sand grains sampled from the base of the Whillans Ice Stream (B), which are dominated by chemical weathering microfeatures similar to those visible on particles that have been crushed and treated with HF acid [*Tulaczyk et al.*, 1998]. Enhanced silicate weathering also help explain the abundance of clay mineral assemblages (e.g., kaolinite and smectite) recovered in marine sediment cores located close to Antarctic ice stream outlets [*Ehrmann et al.*, 1992] that have previously been inferred to reflect long-distance transport of preweathered material [*Ehrmann et al.*, 1992]. This assertion is supported by the presence of kaolinite and smectite in Whillans Ice Stream sediments [*Tulaczyk et al.*, 1998]. If this is the case, there are implications for inferring past glacial influences on marine sedimentary record (i.e., changes in transport versus variations in in situ chemical dissolution).

[14] Fourth, our data reveal that sub-ice sheet environments are highly reactive and dynamic reservoirs of water and solute, with the potential for export to downstream environments. Numerous studies have investigated the global significance of valley glaciers and northern hemisphere ice sheets for global solute fluxes and CO_2 drawdown [*Anderson et al.*, 1997; *Sharp et al.*, 1999; *Hodson et al.*, 2000; *Tranter et al.*, 2002a, 2002b], yet the export of solute from Antarctica remains unquantified, apart from a single study focused on dissolved iron export [*Statham et al.*, 2008]. Figure 2 indicates KIS and BIS pore water features at the end of a spectrum of meltwater chemical compositions, clustering with the other ice sheet meltwaters. These data provide a unique opportunity to estimate potential solute fluxes from the Antarctic Ice Sheet for the first time because they represent the chemistry of sub-ice stream meltwaters before their discharge to the ocean, e.g., via outburst events linked to subglacial lake drainage [*Fricker et al.*, 2007; *Goodwin*, 1988].

[15] We focus our analysis on the peripheral fast-flow areas of the Antarctic Ice Sheet, where basal melting is indicated by accelerated ice flow (>10 m yr^{-1}) and the presence of active subglacial lakes [*Smith et al.*, 2009]. Here, meltwater is likely to have a clear path to the ice margin without undergoing basal freeze-on during export [*Smith et al.*, 2009]. We calculate water and solute fluxes from (1) the "Ice Sheet Interior," where velocities are 10–100 m yr^{-1} [*Bamber et al.*, 2000] and assuming mean basal melt rates of 1.6 mm yr^{-1} [*Joughin et al.*, 2004], and (2) the "Ice Streams," where ice velocities are >100 m yr^{-1} [*Bennett*, 2003]. We define two types of ice stream according to the pattern of basal melting. The Ross Ice Streams are a well-known example of what we term here as "low-melt rate ice" (LMR) streams, where basal melt rates are uniformly <10 mm yr^{-1}. We calculate total solute fluxes from the grounded sector of the Ross Ice Streams, including ice sheet, tributaries, and ice stream components, using published basal melt rates and catchment areas [*Joughin et al.*, 2004]. Pine Island Glacier (PIG) is an example of what we term "high-melt rate" (HMR) ice streams, where a proportion of the bed exhibits unusually high basal melt rates (>10 mm yr^{-1} [*Joughin et al.*, 2003]).

Table 3. Calculations of the Potential Solute and Water Fluxes from Antarctica

	Melt Rate (mm yr^{-1})	Area (10^6 km^2)	Water Flux Q (km^3 yr^{-1})	Annual Specific Discharge (m)	Solute Flux		
					10^6 t yr^{-1}	% of Total Solute Global Flux	t km^{-2} yr^{-1}
Global Riverine Fluxes [*Holland*, 1978]	–	149	4.6×10^4	0.31	2131 (total)	–	24 (mean)
1. "Antarctic Interior" (ice velocity 10–100 m yr^{-1})	1.6	5.0	8.1	1.6×10^{-3}	33	**0.60**	6.6
2. Ross Ice Streams (LMR)	2.1–3.8	0.97	2.4	3×10^{-3}	11	**0.52**	10
3. Pine Island Glacier (2.5% area = HMR)	3.0–500	0.18	2.7	1.5×10^{-2}	10	**0.470**	63
4. Scenario A: Ice Streams	3.00–50.0	7.20	9.60	3.8×10^{-3}	39	**0.71**	6.7–41
5. Scenario B: Ice Streams	3.0–50	7.2	23	9.0×10^{-3}	93	**7**	6.7–41
6. Ice Streams + "Interior" (1 + 4)			18	2.3×10^{-3}	72	**1.3**	9.6
7. Ice Streams + "Interior" (1 + 5)			31	4.1×10^{-3}	130	**2.3**	17

We calculate solute fluxes from the grounded sector of PIG catchment. Here, we use basal melt rates for the strong bed area of 500 mm yr^{-1} (estimated as ~2.5% of the total area of PIG [*Joughin et al.*, 2003]) and assume that basal melt rates over the rest of the PIG catchment are similar to mean values for the Ross Ice Streams [*Joughin et al.*, 2004]. Because the relative proportion of LMR versus HMR ice streams in Antarctica is unknown, we create two scenarios to predict what the overall fast-flow ice stream contribution to Antarctic solute fluxes might be. Areas of fast-flow (>100 m yr^{-1}) presently account for 20% of the total grounded ice sheet area (calculated from *Bamber et al.* [2000]). Scenario A assumes that LMR ice streams account for 90% of the fast-flow area, and HMR comprise the remaining 10%. In scenario B, LMR and HMR ice streams have equivalent areas (i.e., 50% of the total). In both scenarios, we assume that both types of ice stream have rates of solute removal similar to the average values reported for the Ross Ice Streams and PIG (Table 3; values of 10.3 and 63 t km^{-2} yr^{-1}, respectively). Total maximum and minimum estimate solute fluxes are derived for Antarctica by adding the interior ice sheet contribution (Table 3, row 1) to fluxes calculated in scenario A (minimum estimate) and scenario B (maximum estimate).

[16] We use the mean chemical composition (4.1×10^{-3} t m^{-3}) of the KIS and BIS pore waters as an estimate of the total dissolved solute concentration in meltwaters draining the East and West Antarctic Ice Sheets. Water fluxes (m^3) are calculated from basal melt rates integrated over the appropriate area of Antarctica (Table 3), with specific annual water discharge (in m) derived by dividing the annual water flux by the catchment area. The total solute flux (in t yr^{-1}) is the product of the total water flux (in m^3) and the solute concentration (in t m^{-3}). Weathering rates (in t km^{-2} yr^{-1}) are calculated by dividing the total solute flux by the catchment area (in km^2).

[17] Table 3 indicates that the "Antarctic Interior" does not contribute significantly to total global solute fluxes (<1%) and displays low overall rates of chemical weathering (6.6 t km^{-2} yr^{-1}; Table 3). However, these initial calculations exclude solute export from ice stream corridors, where basal melt rates are generally higher [*Joughin et al.*, 2003, 2004]. Our calculated solute fluxes from the Ross Ice Streams (LMR type) and PIG (HMR type) are just a fraction of a percent of the world total, yet rates of solute export from PIG are approximately three times the world average because of the high basal melt rates [*Joughin et al.*, 2003]. We calculate that if 10%–50% of Antarctic Ice Streams were the HMR type, ice stream solute fluxes could be between 39 and 93 × 10^6 t yr^{-1}, respectively (0.7%–1.7% of the global total [*Holland*, 1978]). These figures rise to 72–126 × 10^6 t yr^{-1} (1.3%–2.3% of the global total) with the inclusion of solute fluxes from the Antarctic Interior, which is a similar order of magnitude to values reported from large world rivers (Amazon = 153 × 10^6 t yr^{-1} [*Gaillardet et al.*, 1999]). It is notable that our calculated rates of solute export are several orders of magnitude higher than those for all other glacial and nonglacial systems for the same specific discharge [*Anderson*, 2007]. The potential to significantly affect global weathering rates is likely to be small, but solute and water fluxes to coastal areas of Antarctica could be of local and regional significance. For example, our calculated total meltwater flux is approximately a third of the annual runoff from the Greenland Ice Sheet [*Box et al.*, 2006], while water fluxes from the Ross Ice Streams are of a similar order to those generated by basal melting beneath the Ross Ice Shelf [*Shabtaie and Bentley*, 1987]. Because this subglacial water is likely to be solute-rich (e.g., mean alkalinity concentrations for KIS/BIS pore waters are more than double average values of ~2300 μeq L^{-1} reported for the Ross Sea [*Bates et al.*, 1998]), it could constitute a significant source of solute and alkalinity to Antarctic coastal waters. Better quantification of these processes and their downstream effects awaits more comprehensive data regarding solute concentrations and basal melt rates under ice streams.

[18] In conclusion, ice mass size exerts a critical control on the balance of subglacial biogeochemical processes. We contend that ice sheet beds are driven to anoxia by the microbial oxidation of sulfide minerals and organic carbon, creating a spectrum of Eh/pH microhabitats for microbial colonization and optimal conditions for methanogenesis in the ice sheet interior. Enhanced silicate mineral dissolution liberates key nutrients critical for the survival of microbial communities in these oligotrophic systems, and sulfide oxidation continues to drive dissolution despite the anoxic conditions and potential exhaustion effects. We estimate that solute fluxes from Antarctica are similar to those of the largest rivers on our planet, and rates of chemical weathering are high for the specific discharge. Consequently, export

of this solute to marine embayments could have significance for regional water and solute budgets. These data provide just a glimpse of the new insights into ice sheet biogeochemistry that are certain to emerge during the next decade, as proposed drilling campaigns [*Wadham et al.*, 1998, 2004] delve for the first time into wet-based ecosystems beneath ice sheets.

Appendix A

A1. Engabreen: Fall 2004, Spring 2006, and Fall 2006

[19] Samples were collected directly from subglacial intake pipes bored in bedrock, which feed meltwaters from the glacier bed. Each sample was filtered immediately through 0.45-μm cellulose nitrate filters and stored in polyethylene bottles in the dark for up to 6 months before analysis. The major base cations (Na^+, K^+, Ca^{2+}, and Mg^{2+}) and strong acid anions (SO_4^{2-} and Cl^-) were determined by ion chromatography on the Dionex 4000i Ion Chromatograph System. The precision and accuracy of analyses were within 10%. Alkalinity was determined from the negative deficit of charge balance.

A2. Greenland: Bristol Glacier 2000

[20] Water samples were collected from near the main portal of Bristol Glacier at ~11.00 h daily during a subglacial outburst flood from day of year 179.7 (27 June) through 188 (8 July) in 2000. All water samples were filtered immediately after collection through a 0.45-μm cellulose nitrate membrane filter, using a handheld vacuum pump and Nalgene filter unit. Filtrate for analysis of the major cations and anions was decanted into 20-mL scintillation vials, prerinsed three times with the filtrate before filling. Analysis of the major cations, anions, and dissolved Si was conducted 4–6 months after collection. The major cations and anions were determined by ion chromatography on the Dionex 4000i Ion Chromatograph System. Alkalinity (predominantly HCO_3^-) was determined from the negative deficit of charge balance. The precision of SO_4^{2-}, Cl^-, Ca^{2+}, Mg^{2+}, Na^+, and K^+ analyses was ±0.9%, ±7%, ±0.6%, ±0.2%, ±0.7%, and ±20%, respectively. The accuracy of determinations was −1.6%, +5.9%, −4.8%, −6.6%, −1.9%, and 12.6%, respectively.

A3. Vostok Accretion Ice

[21] Ice cores from 1686, 2334, 2758, 3081, 3537, 3548, 3567, 3569, 3570, 3572, 3573, 3575, 3576, 3578, 3579, 3581, 3582, 3585, 3588, 3591, and 3605 m were obtained from the U.S. National Ice Core Laboratory (Denver, CO), and cores from 3612 and 3622 m were obtained from the Laboratoire de Glaciologie et Géophysique de l'Environment (LGGE) in Grenoble, France. Ice cores were stored in sealed polyethylene tubing at −25°C until analysis. Ice cores used for major ion determinations were cut with a band saw, housed with at −10 °C walk-in freezer, and lightly scraped (at least 0.5 mm from each surface) with a clean razor blade to remove any possible contamination and condensation frozen onto the surface. Only a clean latex glove touched the ice, and new gloves were worn for each sample. Ice samples were transferred to a BioGard vertical laminar flow hood (Model B6000-1; Baker Company) and warmed to room temperature (~20°C) until the surface began to melt (~5 minutes). The ice was then held with clean stainless steel forceps and rinsed thoroughly with 300 mL of 0.2-μm-filtered Barnstead nanopure water. The rinsed ice was placed in a prerinsed Ziploc freezer bag and was allowed to melt completely at room temperature. Samples for major ions were collected from the bags with plastic pipettes and transferred to prerinsed HDPE bottles and stored frozen at −25°C until analysis.

[22] A "control" ice core, prepared by freezing 0.2-μm-filtered nanopure water in a polycarbonate tube and treated in exactly the same way as the Vostok ice core samples, contained very low levels of major ions, close to or below the detection limit (~0.1 μeq L^{-1}), and indicated that background particulate matter contamination represented <20% of the lowest concentration of particulates observed in any of the samples. The migration of the kerosene based drilling fluid into the core was analyzed for selected samples by gas chromatography-mass spectrometry and shown to be negligible.

[23] Ion chromatography was used for major ion determinations. Samples were run through the Dionex DX-120. The eluent flow rate was set to 1.2 mL min^{-1} for both anion and cation analyses. A large sample loop, ~400 μL, was used for all samples and standards. A Dionex IonPac CS12A analytical column (4 × 250 mm) and a CG12A guard column (4 × 50 mm) were used for determining the cations. The eluent was 0.13% methanesulfonic acid solution. An ultra cation self-regenerating suppressor was used. A Dionex IonPac AS14 analytical column (4 × 250 mm) and an AG14 guard column (4 × 50 mm) were used for anion analysis. The eluent was a 1.0 mM $NaHCO_3$ and 3.5 mM Na_2CO_3 solution. An ultra anion self-regenerating suppressor was used.

A4. Midre Lovénbreen (1997–2000)

[24] Samples emerging from upwelling outlets were collected by hand in 1997, 1999, and 2000 and were filtered immediately through 0.45-μm cellulose nitrate filters. All samples were stored airtight in prerinsed 60-mL polyethylene Nalgene bottles and refrigerated awaiting further analysis. Anions of chloride, sulfate, and nitrate were determined on return to the United Kingdom using the Dionex DX 100 Ion Chromatograph System. On the basis of the repeat analysis of reference standard materials, precision was quoted as 0.72%, 3.35%, and 1.19% relative standard deviation (RSD) for nitrate, chloride, and sulfate, respectively. For the 1997 and 1999 samples, total alkalinity (predominantly present as bicarbonate) was determined by titrating with 1 mmol acid (HCl) to an end point pH of 4.5 using BDH mixed indicator. Precision calculated from repeated analysis of the samples was quoted as 5% RSD. In 2000 and 2002, alkalinity was determined from the change balance deficit. Calcium and magnesium were analyzed by atomic absorption spectroscopy. Precision estimates from repeat analysis of the reference standard materials of comparable concentrations to the

samples under analysis were calculated as 0.27% and 2.46% RSD for calcium and magnesium, respectively.

Appendix B: Microbial CO_2 Calculations

[25] We calculate the percentage contribution of microbially derived HCO_3^- ($HCO_{3\text{Microbial}}^-$) to total HCO_3^- for glacier data sets where the intercept of the line of best fit for plots of HCO_3^- versus $*SO_4^{2-}$ was >220 μeq L^{-1} and, hence, cannot be explained by calcite hydrolysis. Hence, this calculation was performed for the glaciers Finsterwalderbreen (1994 and 1997), Midre Lovénbreen (2000 and 2002), and Engabreen (spring 2004). We express the excess HCO_3^- (above the theoretical value of 220 μeq L^{-1} for calcite hydrolysis) as a percentage of the mean HCO_3^- for each glacier data set [equation (B1)], where the mean HCO_3^- is calculated by averaging the HCO_3^- concentrations for each temporally discrete sampling point.

$$\%HCO_{3\text{Microbial}}^- = 100\left[\frac{\text{Intercept}\left(HCO_3^- \text{ versus } SO_4^{2-}\right) - 220}{\text{mean } HCO_3^-}\right] \quad \text{(B1)}$$

We also calculate the total amount of solute generated via microbial CO_2 (assuming that each mole of microbially derived HCO_3^- is balanced by the molar equivalent of cation charge). This quantity is expressed as a proportion ($\%Solute_{Microbial}$) of the total mean solute concentration ($solute_{MEAN}$) for the different glaciers [equation (B2)], where total mean solute concentrations are derived in a similar manner to the HCO_3^- mean concentration.

$$\%Solute_{Microbial} = 100\left[\frac{HCO_3^- \times 2}{(solute)_{MEAN}}\right] \quad \text{(B2)}$$

This excess "microbial" HCO_3^-, on average, accounts for 36% of all HCO_3^- in meltwaters. When added to the equivalent cation charge and expressed as a percentage of total crustal mean solute concentrations, we estimate that, for this data set, 14%–37% of solute is acquired using microbial CO_2.

[26] **Acknowledgments.** This paper was written by J. L. Wadham while on a Phillip Leverhulme Award fellowship. Data have been compiled from 15 years of international research, funded by a variety of sources, including Natural Environment Research Council, United Kingdom; the National Science Foundation, Arlington, VA; the Royal Society; Leverhulme Trust; and the European Union, Brussels, Belgium.

References

Anderson, S. P. (2007), Biogeochemistry of glacial landscape systems, *Annu. Rev. Earth Planet. Sci.*, *35*, 375–399.

Anderson, S. P., J. I. Drever, and N. F. Humphrey (1997), Chemical weathering in glacial environments, *Geology*, *25*(5), 399–402.

Bamber, J. L., D. G. Vaughan, and I. Joughin (2000), Widespread complex flow in the interior of the Antarctic Ice Sheet, *Science*, *287*, 1248–1250.

Bates, N. R., D. A. Hansell, C. Carlson, and L. Gordon (1998), Distribution of CO_2 species, estimates of net community production, and air-sea exchange in the Ross Sea polyna, *J. Geophys. Res.*, *103*(C2), 2883–2986.

Bennett, M. R. (2003), Ice streams as the arteries of an ice sheet: Their mechanics, stability and significance, *Earth Sci. Rev.*, *61*, 309–339.

Bhatia, M., M. Sharp, and J. Foght (2006), Distinct communities exist beneath a high Arctic polythermal glacier, *Appl. Environ. Microbiol.*, *72*(9), 5838–5845.

Bottrell, S. H., and M. Tranter (2002), Sulphide oxidation under partially anoxic conditions at the bed of the Haut Glacier d'Arolla, Switzerland, *Hydrol. Processes*, *16*(12), 2363–2368.

Box, J. E., et al. (2006), Greenland Ice Sheet surface mass balance variability (1988–2004) from calibrated Polar MM5 output, *J. Clim.*, *19*, 2783–2801.

Brown, G. H., M. J. Sharp, M. Tranter, A. Gurnell, and P. W. Nienow (1994), Impact of post-mixing chemical reactions on the major ion chemistry of bulk meltwaters draining the Haut Glacier d'Arolla, Valais, Switzerland, *Hydrol. Processes*, *8*(6), 465–480.

Christner, B., et al. (2006), Limnological conditions in Subglacial Lake Vostok, Antarctica, *Limnol. Oceanogr.*, *51*(6), 2485–2501.

Das, S. I., et al. (2008), Fracture propagation to the base of the Greenland Ice Sheet during supraglacial lake drainage, *Science*, *320*(5877), 778–781.

DeAngelis, M., J. R. Petit, J. Savarino, R. Souchez, and M. H. Thiemens (2004), Contributions of an evaporitic-type reservoir to Lake Vostok chemistry, *Earth Planet. Sci. Lett.*, *222*(3–4), 751–765.

Ehrmann, W. U., M. Melles, G. Huhn, and H. Grobe (1992), Significance of clay mineral assemblages in the Antarctic Ocean, *Mar. Geol.*, *107*, 249–273.

Foght, J., Aislabie S. Turner, C. E. Brown, J. Ryburn, D. J. Saul, and W. Lawson (2004), Culturable bacteria in subglacial sediments and ice from two Southern Hemisphere glaciers, *Microb. Ecol.*, *47*, 329–340.

Föllmi, K., R. Hosein, K. Arn, and P. Steinmann (2009), Weathering and the mobility of phosphorus in the catchments of and forefields of the Rhone and Oberaar glaciers, central Switzerland: Implications for the global phosphorus cycle on interglacial-glacial timescales, *Geochim. Cosmochim. Acta*, *73*, 2252–2282.

Fricker, H. A., T. Scambos, R. Bindshadler, and L. Padman (2007), An active subglacial water system in West Antarctica mapped from space, *Science*, *315*(5818), 1544–1548.

Gaillardet, B. Dupré, P. Louvat, and C. J. Allegré (1999), Global silicate and CO_2 consumption rates deduced from the chemistry of large rivers, *Chem. Geol.*, *159*, 3–30.

Goodwin, I. D. (1988), The nature and origin of a jökulhlaup at Casey Station, Antarctica, *J. Glaciol.*, *34*(116), 95–101.

Hodson, A. J., M. Tranter, and G. Vatne (2000), Contemporary rates of chemical denudation and atmospheric CO_2 sequestration in glacier basins: An Arctic perspective, *Earth Surf. Processes Landforms*, *25*, 1447–1471.

Hodson, A. J., P. N. Mumford, J. Kohler, and P. M. Wynn (2005), The high Artic glacial ecosystem: New insights from nutrient budgets, *Biogeochemistry*, *72*, 233–256.

Hoffman, P. F., A. J. Kaufman, G. P. Halvorsen, and D. P. Shrag (1998), Neoproterozoic Snowball Earth, *Science*, *281*(381), 1342–1346.

Holland, H. D. (1978), *The Chemistry of the Atmosphere and Oceans*, Wiley, New York.

Holloway, J. M., and R. A. Dahlgren (2002), Nitrogen in rocks: Occurrences and biogeochemical implications, *Global Biogeochem. Cycles*, *16*(4), 1118, doi:10.1029/2002GB001862.

Joughin, I., E. Rignot, C. Rosonova, B. Lucchitta, and J. Bohlander (2003), Timing of recent accelerations of Pine Island Glacier, Antarctica, *Geophys. Res. Lett.*, *30*(13), 1706, doi:10.1029/2003GL017609.

Joughin, I., S. Tulaczyk, D. R. MacAyeal, and H. Engelhardt (2004), Melting and freezing beneath the Ross Ice Streams, Antarctica, *J. Glaciol.*, *50*, 168, 96–108.

Lanoil, B., et al. (2009), Bacteria beneath the West Antarctic Ice Sheet, *Environ. Microbiol.*, *11*(3), 609–615.

Mikucki, J., et al. (2009), A contemporary microbially-maintained subglacial ferrous ocean, *Science*, *324*, 397–399.

Priscu, J. C., et al. (2005), Exploring subglacial Antarctic lake environments, *EOS Trans. AGU*, *20*(17), 193–200.

Priscu, J. C., S. Tulaczyk, M. Studinger, M. C. Kennicutt II, B. Christner, and C. Foreman (2008), Antarctic subglacial water: Origin, evolution, and ecology, in *Polar Lakes and Rivers*, edited by W. F. Vincent and J. Laybourn-Parry, pp. 119–136, Oxford Univ. Press, Oxford, UK.

Raiswell, R., et al. (2006), Contributions from glacially derived sediment to the global iron(oxyhydroxide) cycle: Implications for iron delivery to the oceans, *Geochim. Cosmochim. Acta*, *70*, 2765–2780.

Raiswell, R., L. Benning, M. Tranter, and S. Tuylacyzk (2008), Bioavailable iron in the Southern Ocean: Significance of the iceberg conveyor belt, *Geochem. Trans.*, *9*, 7, doi:10.1186/1467-4866-9-7.

Raiswell, R., L. G. Benning, L. Davidson, M. Tranter, and S. Tulaczyk (2009), Schwertmannite in wet, acid and oxic microenvironments beneath polar and polythermal glaciers, *Geology*, *37*, 431–434.

Shabtaie, S., and M. Bentley (1987), West Antarctic Ice Streams draining into the Ross Ice Shelf: Configuration and mass balance, *J. Geophys. Res.*, *92*(B2), 1311–1336.

Sharp, M. J., M. Tranter, G. H. Brown, and M. Skidmore (1995), Rates of chemical denudation and CO_2 drawdown in a glacier-covered alpine catchment, *Geology*, *23*, 61–64.

Sharp, M. J., J. Parkes, B. Cragg, I. J. Fairchild, H. Lamb, and M. Tranter (1999), Widespread bacterial populations at glacier beds and their relationship to rock weathering and carbon cycling, *Geology*, *27*(2), 107–110.

Siegert, M. J., et al. (2007), Exploration of Ellsworth Subglacial Lake: A concept paper on the development, organisation and execution of an experiment to explore, measure and sample the environment of a West Antarctic subglacial lake, *Rev. Environ. Sci. Biotechnol.*, *6*(1–3), 161–179.

Skidmore, M., J. Foght, and M. J. Sharp (2000), Microbial life beneath a High Arctic glacier, *Appl. Environ. Microbiol.*, *66*(8), 3214–3220.

Skidmore, M., S. P. Anderson, M. J. Sharp, J. M. Foght, and B. D. Lanoil (2005), Comparison of microbial community composition in two subglacial environments reveals a possible role for microbes in chemical weathering processes, *Appl. Environ. Microbiol.*, *71*(11), 6986–6997.

Skidmore, M., M. Tranter, S. Tulaczyk, and B. Lanoil (2010), Hydrochemistry of ice sheet beds – Evaporitic or microbial effects?, *Hydrol. Processes*, in press.

Smith, B. E., H. Fricker, I. R. Joughin, and S. Tulaczyk (2009), An inventory of active subglacial lakes in Antarctica detected by ICESat (2003–2008), *J. Glaciol.*, *55*(192), 573–595.

Statham, P. J., M. Skidmore, and M. Tranter (2008), Inputs of glacially derived dissolved and colloidal iron to the coastal ocean and implications for primary productivity, *Global Biogeochem. Cycles*, *22*(3), GB3013, doi:10.1029/2007GB003106.

Thoma, M., K. Grosfeld, and C. Meyer (2008), Modelling accreted ice in subglacial lake Vostok, *Geophys. Res. Lett.*, *35*, L11504, doi:10.1029/2008GL033607.

Tranter, M., M. J. Sharp, H. R. Lamb, G. H. Brown, B. P. Hubbard, and I. C. Willis (2002a), Geochemical weathering at the bed of the Haut Glacier d'Arolla: A new model, *Hydrol. Processes*, *16*, 959–993.

Tranter, M., et al. (2002b), Direct effect of ice sheets on terrestrial bicarbonate, sulphate and base cation fluxes during the last glacial cycle: Minimal impact on atmospheric CO_2 concentrations, *Chem. Geol.*, *190*(1–4), 33–44.

Tranter, M., M. Skimore, and J. L. Wadham (2005), Hydrological controls on microbial communities in subglacial environments, *Hydrol. Processes*, *19*, 995–998.

Tulaczyk, S., B. Kamb, R. P. Scherer, and H. Engelhardt (1998), Sedimentary processes at the base of a West Antarctic Ice Stream: Constraints from textual and compositional properties of subglacial debris, *J. Sediment. Res.*, *68*(3), 487–496.

Wadham, J. L., A. J. Hodson, M. Tranter, and J. A. Dowdeswell (1998), The hydrochemistry of meltwaters during the ablation season at a High Arctic, polythermal-based glacier, south Svalbard, *Hydrol. Processes*, *12*, 1825–1849.

Wadham, J. L., S. Bottrell, M. Tranter, and R. Raiswell (2004), Stable isotope evidence for microbial sulphate reduction at the bed of a polythermal high Arctic glacier, *Earth Planet. Sci. Lett.*, *219*, 341–355.

Wadham, J. L., M. Tranter, S. Tulaczyk, and M. Sharp (2008), Subglacial methanogenesis: A potential climatic amplifier?, *Global Biogeochem. Cycles*, *22*, GB2021, doi:10.1029/2007GB002951.

Weitemeyer, K., and B. A. Buffett (2008), Accumulation and release of methane from clathrates from below the Laurentide and Cordilleran ice sheets, *Global Planet. Change*, *53*, 176–187.

Wingham, D., M. J. Siegert, A. Shepherd, and A. S. Muir (2006), Rapid discharge connects Antarctic subglacial lakes, *Nature*, *440*, 1033–1036.

Wynn, P. M., A. J. Hodson, and T. Heaton (2006), Chemical and isotopic switching within the subglacial environment of a high Arctic glacier, *Biogeochemistry*, *78*, 173–193.

Zwally, H. J., W. Abdulati, T. Herring, K. Larson, J. Scaba, and K. Steffen (2002), Surface melt-induced acceleration of Greenland Ice Sheet flow, *Science*, *297*(5579), 218–222.

A. J. Hodson, Department of Geography, University of Sheffield, Sheffield S10 2TN, UK.

M. Jackson, Glacier and Environmental Hydrology Section, Hydrology Department, Norwegian Water Resources and Energy Directorate, P.O. Box 5091 Maj, N-0301 Oslo, Norway.

W. B. Lyons, Byrd Polar Centre, Ohio State University, 1090 Carmack Rd., Scott Hall, Columbus, OH 43210, USA.

J. Priscu, Department of Land Resources and Environmental Science, Montana State University, Bozeman, MT 59717, USA.

M. Sharp, Department of Earth and Atmospheric Sciences, University of Alberta, 1-26 Earth Science Bldg., Edmonton, Alberta, AB, Canada.

M. Skidmore, Department of Earth Sciences, Montana State University, Bozeman, MT 59717, USA.

M. Tranter and J. L. Wadham, Bristol Glaciology Centre, School of Geographical Sciences, University of Bristol, University Road, Bristol BS8 1SS, UK. (j.l.wadham@bris.ac.uk)

P. Wynn, The Lancaster Environment Centre, Lancaster University, Lancaster LA1 4YQ, UK.